ACADÉMIE
DES SCIENCES
INSTITUT DE FRANCE

Comptes Rendus
Chimie

Mourad Makhlouf, Hichem Hachemi, Meriem Boutamine, Zoubir Benmaamar and Didier Villemin

Recycling graphite waste for high-performance nanofluids: synthesis and property analysis

Volume 29 (2026), p. 397-406

Online since: 17 August 2026

https://doi.org/10.5802/crchim.424

The Comptes Rendus. Chimie *are a member of the Mersenne Center for open scientific publishing*
www.centre-mersenne.org — e-ISSN : 1878-1543

ACADÉMIE DES SCIENCES
INSTITUT DE FRANCE

Comptes Rendus. Chimie
2026, Vol. 29, p. 397-406
https://doi.org/10.5802/crchim.424

Research article

Recycling graphite waste for high-performance nanofluids: synthesis and property analysis

Mourad Makhlouf[*,a,b], **Hichem Hachemi**[a], **Meriem Boutamine**[a], **Zoubir Benmaamar**[b] **and Didier Villemin**[c]

[a] Scientific and Technological Research Directorate-Cherchell Academy DPHB, Tipaza, Algeria

[b] Laboratory of Energy Processes and Nanotechnology, University of Blida-Algeria, Algeria

[c] Laboratory of Molecular and Thio-organic Chemistry, UMR CNRS 6507, INC3M, FR 3038, ENSICAEN and Research Center, University of Caen, France

E-mail: makhlouf_mourad@univ-blida.dz (M. Makhlouf)

Abstract. Graphene, a remarkable material with extraordinary properties, has revolutionary potential for various technological applications. However, conventional methods of graphene production often involve energy-intensive and polluting processes. To address this challenge, we propose a sustainable approach that combines the production of high-quality graphene from recycled battery waste and its integration into nanofluids. Thanks to a simple and scalable electrochemical exfoliation technique, it is possible to obtain graphene with superior properties. The present study focuses on the large-scale preparation of graphene by recycling graphite from energy storage devices using a simple and inexpensive electrochemical technique. Characterization of the obtained materials was carried out by Raman spectroscopy, X-ray diffraction, specific surface area analysis, and scanning electron microscopy. The viscosity measurement and analysis of a graphene–water nanofluid were carried out at different temperatures and volume fractions. All viscosity measurements were carried out using a capillary viscometer at temperatures between 25 and 65 °C. The nanofluid showed increasing viscosity with increasing nanoparticle concentration and decreasing viscosity with increasing temperature.

Keywords. Graphene, Recycling, Graphite, Electrochemical exfoliation, Nanofluid.

Note. Publication delayed at the request of the author.

Manuscript received 1 May 2025, revised 12 September 2025, accepted 18 September 2025, online since 17 August 2026.

1. Introduction

Graphene has demonstrated excellent mechanical [1], thermal [2], optical, and electronic properties [3], offering the potential for a range of applications in energy storage [4], catalysis [5], sensing [6], molecular separation [7], and protective composite coatings [8]. However, producing graphene in an environmentally friendly and cost-effective way remains a significant challenge [9]. One promising solution is the electrochemical exfoliation of graphite, which requires an electrolyte containing intercalation species, a graphite electrode as a source of graphene, and a power supply [10]. One approach that addresses these concerns is the utilization of recycled graphite waste as a sustainable and cost-effective source of graphene [11]. Other research has explored using graphene and graphene oxide, synthesized economically via the modified Hummers method, in battery manufacturing [12–14].

[*] Corresponding author

Efficient graphite exfoliation into graphene depends on both anion intercalation and water oxidation. Sulfate anions, due to their strong binding energy and reversible behavior, facilitate the entry of water into the graphite, which makes the exfoliation more effective [15]. Gupta et al. [16] demonstrated that the materials' electrical properties enable an open-circuit voltage of around 250 mV and a maximum power of 22 μW. This study suggests that graphene oxide could be a cost-effective material for producing compact energy devices, highlighting its potential in the field of microbatteries. Commonly used anionic intercalation species include sulfate (SO_4^{2-}) [17], perchlorate (ClO_4^-) [18], trifluoroborate (BF_4^-) [19], and hexafluorophosphate (PF_6^-) [20]. Sulfate is one of the most commonly used anions. It is highly effective in facilitating the exfoliation process in aqueous solutions of acidic or neutral inorganic salts, including those containing sulfuric acid and ammonium sulfate [21]. Graphene has emerged as a potential leader in the development of high-performance nanofluids thanks to its unique mechanical, thermal, and electrical properties [22,23]. Even at low concentrations, graphene sheets are known to enhance thermal conductivity, enabling the development of high-performance cooling technologies, particularly for electronic devices [24,25]. Furthermore, graphene can stabilize nanofluids by forming a protective layer around most of the released nanoparticles [26].

Nanofluids have found numerous scientific and industrial applications [27,28]. However, due to their highly complex nature, predicting the thermophysical properties of these fluids has become a major research challenge [29,30]. Some studies on the rheological behavior of nanofluids have focused on determining whether they are Newtonian or non-Newtonian fluids [31]. However, many factors influence the viscosity of nanofluids, such as temperature, pH, volume fraction, particle size, particle size distribution, zeta potential, and base fluid [32–34]. The influence of nanofluid viscosity on nanoparticle loading has been extensively studied [35–37]. The viscosity of nanofluids containing various types of nanoparticles, such as metals, oxides, and carbon nanotubes, has been studied as a function of nanoparticle concentration [38,39]. Despite extensive experimental studies on the effect of nanoparticle loading on nanofluid viscosity, there is no universal equation that can predict this property with any great accuracy [40,41]. Furthermore, almost all studies on nanofluid viscosity have demonstrated a positive correlation between viscosity and increasing nanoparticle volume fraction [42,43]. However, this has not been observed in all nanofluids, except for those based on carbon nanotubes, which exhibit an inverse relationship between viscosity and particle loading [44]. Moreover, Nadooshan et al.'s comprehensive study of the rheological behavior of nanofluids concluded that most nanofluids exhibit Newtonian behavior at low volume fractions and non-Newtonian behavior at high nanoparticle volume fractions [45]. Additionally, an increase in volume fraction has been shown to lead to nanoparticle aggregation and consequently an increase in fluid viscosity [46,47]. This increase in viscosity is due to the increase in the surface/volume ratio during aggregate formation [48,49]. The effect of aggregation on the viscosity of Al_2O_3–water nanofluids was studied, and the results confirmed that relative viscosity increases with increasing aggregate formation. The results also showed that the nanofluid's volume fraction does not directly affect viscosity and that an increase in particle loading leads to aggregate formation. Consequently, viscosity increases with aggregation size [50]. However, research into the effect of temperature on the viscosity of nanofluids has not resulted in a universal formula describing the viscosity behavior of these complex fluids as a function of temperature [51,52]. This may be because other factors, such as the type of base fluid, volume fraction, and particle size, affect the viscosity [53].

Consequently, relative viscosity ($\mu_{rel} = \mu_{nanofluid}/\mu_{basefluid}$) has been found to be more advantageous than absolute viscosity, as this makes it easier to understand the temperature dependence of viscosity [54]. Relative viscosity remained virtually stable with increasing temperature for low to moderate particle loading for almost all nanofluid types. However, at high nanoparticle concentrations, relative viscosity began to grow with temperature [55]. A few studies have shown hysteresis of nanofluid relative viscosity with temperature, where relative viscosity increases and decreases with temperature [56]. This behavior was observed in the study by Namburu et al. [57]. Other researchers have concluded that relative viscosity decreases with increasing temperature. The study by Li et al. [58]

on zinc oxide nanoparticles dispersed in ethylene glycol (ZnO-EG nanofluids) demonstrates a clear correlation between nanoparticle size, volume fraction, and the resulting relative viscosity of the suspension. Most studies on the influence of nanoparticle size have shown a decrease in viscosity as the particle size increases. Viscosity of the water–graphene nanofluid increases with nanoparticle concentration and decreases with temperature. Surface tension also decreases in both cases [59,60]. Other studies [61] have demonstrated a direct relationship between viscosity and nanoparticle size. Ahammed et al. have explored how varying volume concentration and temperature influences the viscosity and surface tension of a water–graphene nanofluid. Their results demonstrate that viscosity is more sensitive to volume concentration than to temperature, indicating its potential as an effective coolant for real-time thermal applications [62]. The novelty of our study lies in its sustainable and economical approach to producing high-quality graphene. Rather than using conventional methods that are energy-intensive and polluting, our research proposes recycling graphite from battery waste using a simple, low-cost, electrochemical exfoliation technique.

2. Experimental section

2.1. *Synthesis of graphene*

High-quality, large-area graphene sheets were produced by synthesizing graphene through electrochemical exfoliation of graphite rods from used electric batteries. These rods act as electrodes, serving as both the anode and the cathode in an aqueous solution of sulfuric acid (H_2SO_4). Applying a constant direct current voltage of 10 V to the electrodes initiated an electrochemical reaction that intercalated sulfate ions into the graphite layers. This intercalation process expanded the graphite structure, resulting in its exfoliation into graphene sheets. The process typically required 1.5 h to completely consume the graphite anode. The aqueous electrolyte of graphene was then subjected to centrifugation at 10 000 tr/min for 5 min and the pellet washed multiple times with distilled water to remove residual acid and impurities. A 1:10 (w/v) solid-to-liquid ratio was used during the washing steps. After undergoing a half-hour sonication process, the graphene was dried under vacuum for 24 h at 333 K [8].

2.2. *Characterization of graphene*

The microscopic morphology of the samples was characterized using scanning electron microscopy (SEM on a Quanta FEG 250). The materials' structures were characterized by Fourier transform infrared spectroscopy (FT-IR on a JASCO V 770 spectra analyzer), X-ray diffraction (XRD on a D8 Advance Eco Bruker diffractometer, which operated using a copper tube at λ = 1.54 Å). Raman spectroscopy was also used (inVia from Renishaw, with monochromatic Ar^+ laser radiation at a wavelength of 514.5 nm). A BET analyzer (Gemini VII 4.00) was used to determine the materials' specific surface area, pore size, and volume. The specific surface area was determined by relating the amount of nitrogen adsorbed to the nitrogen pressure. These parameters were calculated using the Brunauer–Emmett–Teller (BET) and Barrett–Joyner–Halenda (BJH) methods.

2.3. *Preparation of nanofluid*

Nanofluids were prepared by dispersing the exfoliated graphene in deionized water (as the base fluid), achieving a uniform and homogeneous dispersion. The density of graphene is 2.1 g/cm^3. In its natural state, graphene exists as sheets with a two-dimensional structure. It has excellent mechanical, thermal, and electrical properties. However, its dispersion is complex due to its large specific surface area. The use of high-power ultrasonic equipment enabled the dispersion of graphene. The results show the consistency and stability of the nanofluid. Five samples of graphene–deionized water were prepared with different concentrations (0.001, 0.002, 0.003, 0.004, and 0.005 g/L). All prepared samples were then subjected to ultrasonication (200 W, 20 to 40 kHz) for approximately 2 h at room temperature to ensure homogeneity and stability. To ensure the stability and reproducibility of the viscosity measurements, samples stored for extended periods were re-dispersed via ultrasonication for 30 to 60 min prior to analysis.

3. Results and discussion

Scanning electron microscopy (SEM) is an excellent technique for studying the micro- and/or nanostructure, topography, and distribution of different phases in samples. Figure 1 shows images of graphene at different magnifications: 200, 12 000 and 24 000×.

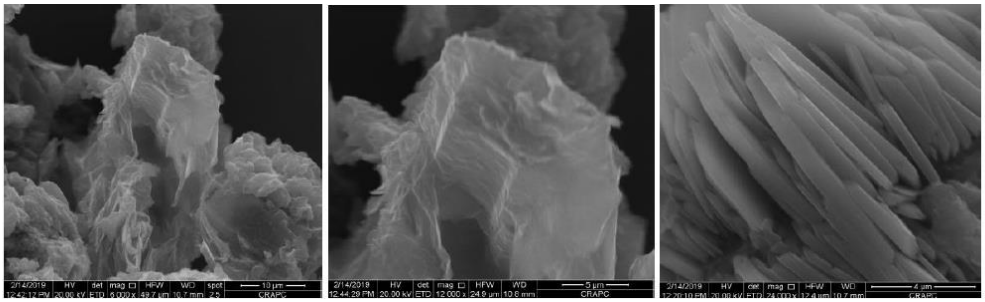

Figure 1. SEM of graphene [10] (© 2022 IOP Publishing. Reproduced with permission. All rights reserved).

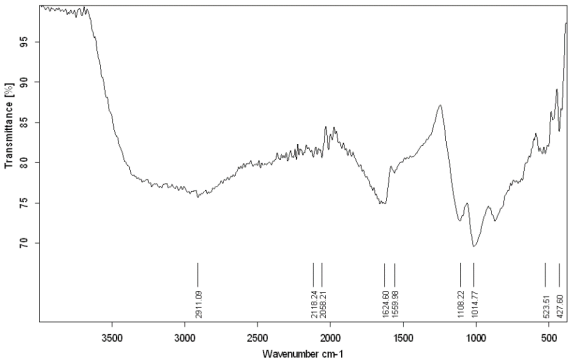

Figure 2. FT-IR of graphene.

The SEM images in Figure 1 confirm the exfoliation of the graphite into multi-layered graphene sheets, which are entangled due to their overlap. They also show a smooth structure for the synthesized graphene.

The FTIR spectrum of graphene (Figure 2) shows a broad band centered around 3500–2800 cm^{-1}, which is characteristic of O–H stretching vibrations. This indicates the presence of adsorbed water molecules and hydroxyl groups [62]. The band at 1559 cm^{-1} is assigned to the stretching and bending modes of water molecules. The peak at 1624 cm^{-1} corresponds to the aromatic C=C sp^2 stretching vibration. The band at 1014 cm^{-1} corresponds to the C–O of the alkyl groups.

X-ray diffraction (XRD) is the gold standard for characterizing crystalline materials. The XRD patterns of graphite and synthesized graphene are shown in Figure 3.

Analysis by XRD enables the determination of crystal lattice parameters, including interplanar spacing. The XRD pattern provides crucial information on the degree of exfoliation, the number of layers, and the extent of structural order or disorder in graphite-derived carbon materials. The most striking feature of the graphite XRD pattern (Figure 3a) is the sharp, intense peak at approximately $2\theta = 26.5°$. The (002) interlayer spacing of graphite is usually around 0.335 nm. The sharpness of this peak indicates a high degree of crystallinity and long-range order in the stacked layers. Following electrochemical exfoliation to produce graphene, the XRD pattern exhibits a sharp peak at $2\theta = 23°$, which corresponds to the (002) interlayer spacing of the graphene sheets. An additional peak at $2\theta = 44.9°$ is attributed to the (100) planes [63]. The decreased intensity of all diffraction peaks indicates a decrease in the crystallinity of graphite after exfoliation. The increased interlayer distance (d) in the synthesized graphene indicates the intercalation of oxygen-containing functional groups between the layers, confirming the successful formation of graphene [64]. These results demonstrate the structural rearrangements from graphite to graphene.

Raman spectroscopy is a powerful, non-destructive technique used to analyze the molecular composition and structural properties of materials. It is widely used to characterize sp^2 and sp^3 hybridized carbon atoms. The Raman spectra of graphene typically exhibit three distinctive peaks known as the D, G, and 2D bands. The G band arises from the in-plane vibration of sp^2 hybridized carbon atoms in the graphitic lattice and is sensitive to strain and defects. The D band is associated with structural defects and disorder in the sp^2 carbon network. The intensity ratio of the D and G bands is often used as a quantitative measure of disorder, providing insight into the quality of graphene. Figure 4 shows

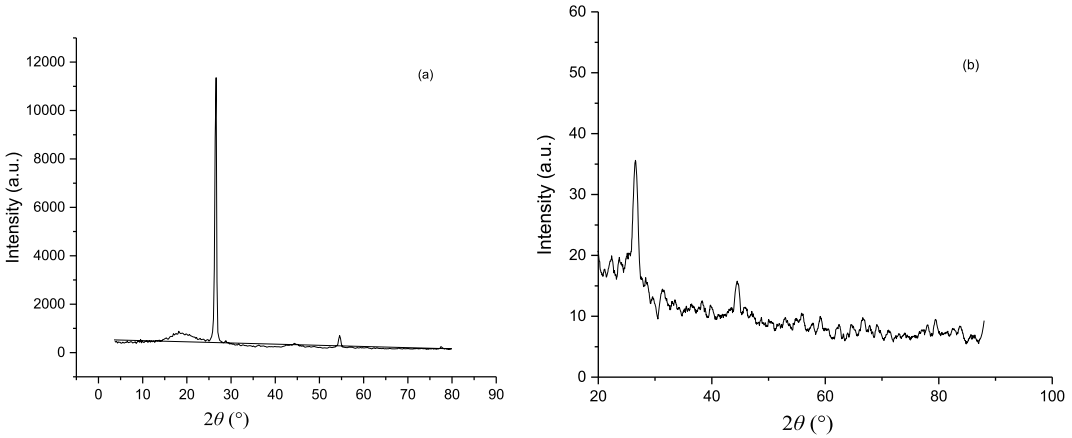

Figure 3. The XRD of (a) graphite and (b) graphene (reproduced with permission from [8]).

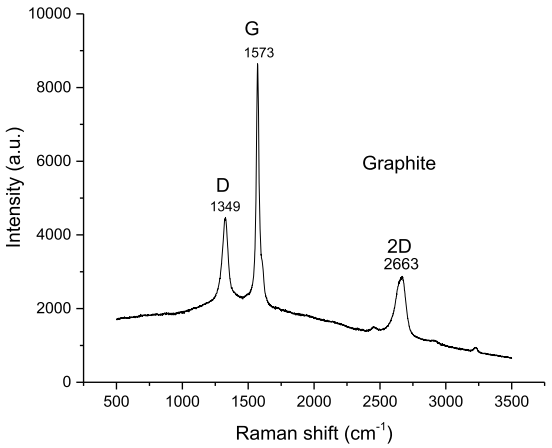

Figure 4. Raman spectrum of graphite (reproduced from [67] under license CC BY-NC-SA 4.0).

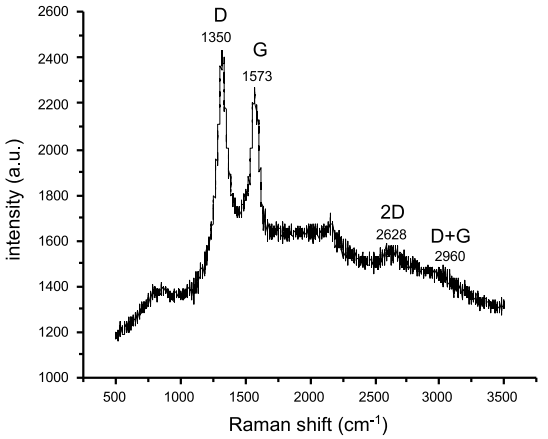

Figure 5. Raman spectrum of graphene (reproduced from [67] under license CC BY-NC-SA 4.0).

the Raman spectrum of graphite, with the characteristic D and G bands appearing at 1349 cm^{-1} and 1573 cm^{-1}, respectively. Additionally, a 2D band is observed at 2663 cm^{-1}, arising from a double resonance process involving two phonons [65,66].

Figure 5 shows the Raman spectrum of graphene, which exhibits four prominent peaks in the 1300–3300 cm^{-1} region at 1328 and 1574 cm^{-1}. The peak at 1328 cm^{-1} is attributed to the D band, the one centered at 1574 cm^{-1} to the G band.

The I_D/I_G intensity ratio of the D and G bands is a quantitative measure of defect density in the graphene lattice. An increase in disorder within the graphene structure leads to a corresponding increase in the I_D/I_G ratio due to increased elastic scattering from defects. However, in highly amorphous carbon materials, the I_D/I_G ratio tends to decrease. The tabulated data below (Table 1) summarize the Raman analysis results for graphite and graphene.

The I_D/I_G ratio was found to be 0.52 for graphite and 1.07 for graphene. This increase suggests a reduction in sp^2 domain size and the incorporation of oxygen-containing functional groups during exfoliation, resulting in greater disorder at carbon edges due to extensive oxidation [44]. To quantify the specific surface area of graphene, nitrogen (N_2) adsorption–desorption isotherms were measured and are shown in Figure 6.

Table 1. Raman analysis values of different materials

Sample	D Position (cm^{-1})	D Intensity (a.u.)	G Position (cm^{-1})	G Intensity (a.u.)	I_D/I_G
Graphite	1328	4411	1573	8565	0.52
Graphene	1322	2427	1573	2260	1.07

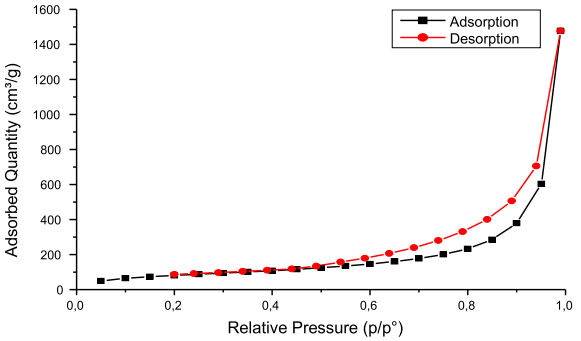

Figure 6. Nitrogen adsorption–desorption isotherm of graphene.

Table 2. BET and BJH analysis results

Sample	S_{BET} (m^2/g)	$S_{Langmuir}$ (m^2/g)	S_{BJH} (m/g)	V_P (cm^3/g)	D_P (Å)
Graphene	300.312	771.768	354.89	0.588	65.05

V_P: Pore volume (cm^3/g); D_P: Pore diameter (Å).

According to the IUPAC classification, the isotherm of graphene is classified as type IV, indicating capillary condensation within the mesopores. The increase in adsorbed volume within the relative pressure range of 0.7–1.0 is attributed to capillary condensation, which is accompanied by a hysteresis loop. The specific surface area, pore volume, and pore size distribution were determined using the BET and BJH methods and are summarized in Table 2.

The specific surface area of graphene usually ranges from 200 to 2500 m^2/g, depending on the preparation method and the extent of exfoliation. Our graphene sample exhibited an S_{BET} of 300.3126 m^2/g, which is attributed to the presence of larger, stacked graphene sheets. The higher Langmuir surface area of 771.768 m^2/g highlights the sensitivity of the method to smaller surfaces. Using the BJH method, we determined a surface area of 354.89 m^2/g, which suggests that there is significant stacking of graphene sheets. The BJH method is particularly sensitive to larger pores. The pore volume (VP) was found to be 0.588 cm^3/g, which also indicates substantial stacking of graphene layers.

4. Viscosity measurements

Viscosity was measured using a Cannon–Fenske capillary viscometer. The viscosity of the graphene-based nanofluids was determined at the lowest concentrations. A thermostatic bath was used to control the ambient temperature. The viscosity of all nanofluids was measured at temperatures of 25, 35, 45, 55, and 65 °C.

The experimental flow time was converted into kinematic viscosity (ν) using the viscometer constant (C), according to the following equation:

$$\nu = C \times t_f$$

where ν is the kinematic viscosity (expressed in centistokes cSt), C is the calibration constant of the specific capillary used (cSt/s), and t_f is the efflux time (s) required for the meniscus to pass between the two calibrated marks. Furthermore, the dynamic viscosity (μ), which represents the fluid's internal resistance to shear, was derived by considering the suspension's density (ρ): $\mu = \nu \cdot \rho_{bulk}$. In this study, the bulk density (ρ_{bulk}) of the nanofluids (expressed in g/cm^3) was measured at each temperature point to account for the thermal expansion of the base liquid and the presence of the graphene nanosheets.

The results of the viscosity measurements are shown in Figure 7.

Figure 7 shows how the viscosity of five graphene-based nanofluids changes with temperature at different concentrations. The measurements were carried out at five specific temperatures: 25, 35, 45, 55, and 65 °C. As expected, viscosity decreases with increasing temperature. Conversely, viscosity increases with the concentration of graphene nanoparticles.

Table 3. Comparative synthesis of results for graphene-based nanofluids: Impact of concentration and temperature

Concentration range	Temperature range (K)	Key results/remarks	Reference
0.03 wt%	298–348	Viscosity lower than that of the base fluid and decreases from 217.4 to 40.6 cP as the temperature increases from 298 to 348 K.	[68]
0.5–1 wt%	278–298	$\mu_{nanofluid}$ decreased with rising temperature but increased with the mass fraction of graphene nanoparticles. μ_{rel} ranged from 1.24 to 2.35.	[69]
0.025–0.1 wt%	293–333	μ decreases 4–44% with rising T and increases with the concentration of graphene nanoparticles. μ_{rel} increases with rising T.	[70]
0.025–0.1 wt%	293–333	Viscosity decreases for higher temperatures and increases for higher concentrations of graphene nanoparticles (+44% compared to the viscosity of the base fluid for 0.1 wt% graphene nanoparticles).	[71]
0.05–0.1 wt%	293–333	Viscosity increases with concentration and decreases with temperature.	[72]
0.001–0.005 g/L	298–333	A decrease in viscosity was observed with increasing temperature. Conversely, viscosity increased with the graphene nanoparticle concentration.	This work

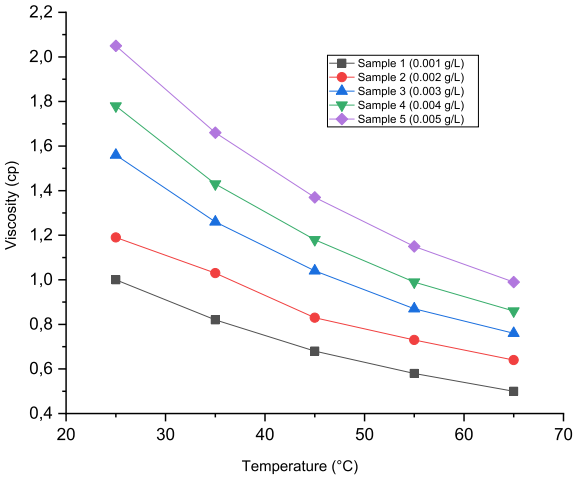

Figure 7. Viscosity measurements of graphene samples.

Increasing temperature promotes the thermal agitation of molecules, thereby increasing their kinetic energy. This weakens the intermolecular attractive forces, thereby reducing the fluid's internal resistance to flow.

A comparative summary of the results obtained for graphene-based nanofluids is provided in Table 3.

This table shows that the viscosity behavior of graphene-based nanofluids can be predicted and is governed by well-established physical laws, even when different base fluids and concentrations are used. Our results are in perfect agreement with those in the scientific literature, which lends credibility and importance to our contribution to the field.

5. Conclusion

We present a method of synthesizing graphene through the electrochemical exfoliation of graphite derived from recycled batteries. Sulfuric acid and water were used as electrolytes to enhance exfoliation. Graphene was then dispersed into individual sheets of graphene using ultrasonic treatment in distilled water. The synthesized graphene was characterized using various techniques, confirming the successful production of high-quality graphene. This study focused on measuring the viscosity and conducting a behavioral analysis of graphene-based nanofluids. The viscosity of the nanofluids was measured at different volume fractions ranging from 0.001 to 0.005. All viscosity measurements were performed using a capillary viscometer at temperatures ranging

from 25 to 65 °C. The studied nanofluids exhibited an increase in viscosity with nanoparticle loading and a decrease with temperature.

Declaration of interests

The authors do not work for, advise, own shares in, or receive funds from any organization that could benefit from this article, and have declared no affiliation other than their research organizations.

References

[1] C. Lee, X. Wei, J. W. Kysar and J. Hone, "Measurement of the elastic properties and intrinsic strength of monolayer graphene", *Science* **321** (2008), pp. 385–388.

[2] J. Li, J. Liu, N. Li, W. Zeng, M. Chen and Y. Xu, "High thermal conductivity graphene-based interfacial materials through oriented assembly and catalytic graphitization for thermal management", *Carbon* **235** (2025), article no. 120081.

[3] P. Kalpana Devi and K. K. Singh, "Enhancement of electronic and optical characteristics of graphene by doping with transition metals – DFT method", *Physica B* **669** (2023), article no. 415309.

[4] A. G. Olabi, M. A. Abdelkareem, T. Wilberforce and E. T. Sayed, "Application of graphene in energy storage device – A review", *Renew. Sust. Energ. Rev.* **135** (2021), article no. 110026.

[5] M. B. Burkholder, F. B. A. Rahman, E. H. Chandler, J. R. Regalbuto, B. F. Gupton and J. M. M. Tengco, "Metal supported graphene catalysis: A review on the benefits of nanoparticular supported specialty sp2 carbon catalysts on enhancing the activities of multiple chemical transformations", *Carbon Trends* **9** (2022), article no. 100196.

[6] M. Boutamine, Y. Bakha, M. Makhlouf, et al., "Graphene concentration effect on the structural and morphological properties of ZnO/G nanocomposites", *J. Mater. Sci. Mater. Electron.* **36** (2025), article no. 15394.

[7] S. Bouriche, M. Makhlouf, M. Kadari, H. Bakli, Y. Hamoumi, B. Benaicha, A. Taibi and Z. Benmaamar, "Smart membrane absorbing electromagnetic waves based on polyvinyl chloride/graphene composites", *Mater. Res. Express* **9** (2022), article no. 045703.

[8] N. Tekkouk, M. Makhlouf, A. Kirad, M. Meziane and S. Aguib, "Effect of graphene nanoparticle incorporation on hard anodizing performance of Al–Cu–Mg aluminum alloy", *Phys. Met. Metallogr.* **126** (2025), pp. 519–527.

[9] C. Jia, M. Pang, Y. Lu, et al., "Graphene environmental footprint greatly reduced when derived from biomass waste via flash Joule heating", *One Earth* **5** (2022), pp. 1394–1403.

[10] H. Bakli, M. Moualhi and M. Makhlouf, "High-sensitivity electrical properties measurement of graphene-based composites using interferometric near-field microwave technique", *Meas. Sci. Technol.* **33** (2022), article no. 045012.

[11] M. Makhlouf, Z. Benmaamar, D. Villemin and T. Tayebi, "Development of graphene oxide nanofluids from recycled graphite: Part I—Materials characterization", *J. Nanofluids* **13** (2024), pp. 967–972.

[12] S. Tripathi, N. Gangwar, C. Gangwar and R. K. Shukla, "Enhanced humidity sensing using graphene oxide and reduced graphene oxide synthesized via modified Hummers' method", *Sens. Imaging* **26** (2025), article no. 20.

[13] X. Wu, H. Xu, Y. Shen, P. Xu, L. Lu, J. Fu and H. Zhao, "Treatment of graphite felt by modified Hummers method for the positive electrode of vanadium redox flow battery", *Electrochim. Acta* **138** (2014), pp. 264–269.

[14] N. Méndez-Lozano, F. Pérez-Reynoso and C. González-Gutiérrez, "Eco-friendly approach for graphene oxide synthesis by modified Hummers method", *Materials* **15** (2022), article no. 7228.

[15] H. Lee, J. I. Choi, J. Park, S. S. Jang and S. W. Lee, "Role of anions on electrochemical exfoliation of graphite into graphene in aqueous acids", *Carbon* **167** (2020), pp. 816–825.

[16] R. K. Gupta, Z. A. Alahmed and F. Yakuphanoglu, "Graphene oxide based low cost battery", *Mater. Lett.* **112** (2013), pp. 75–77.

[17] T. Enoki, M. Endo and M. Suzuki, *Graphite Intercalation Compounds and Applications*, vol. 10, Oxford University Press: Oxford, 2003.

[18] A. Yoshida, Y. Hishiyama and M. Inagaki, "Exfoliated graphite from various intercalation compounds", *Carbon* **29** (1991), pp. 1227–1231.

[19] H. Wang and X. Chen, "A comprehensive review of predicting the thermophysical properties of nanofluids using machine learning methods", *Ind. Eng. Chem. Res.* **61** (2022), pp. 14711–14730.

[20] H. Wang and M. Yoshio, "Suppression of PF_6^- intercalation into graphite by small amounts of ethylene carbonate in activated carbon/graphite capacitors", *Chem. Commun.* **46** (2010), pp. 1544–1546.

[21] D. Zhang, L. Cui, H. Zhu, R. M. A. Madani and J. Liang, "Treatment performance and microbial community under ammonium sulphate wastewater in a sulphate reducing ammonium oxidation process", *Environ. Technol.* **42** (2020), pp. 2982–2990.

[22] M. Sandhya, D. Ramasamy, K. Sudhakar, et al., "A systematic review on graphene-based nanofluids application in renewable energy systems: Preparation, characterization, and thermophysical properties", *Sustain. Energy Technol. Assess.* **44** (2021), article no. 101058.

[23] T. Le Ba, O. Mahian, S. Wongwises and I. M. Szilágyi, "Review on the recent progress in the preparation and stability of graphene-based nanofluids", *J. Therm. Anal. Calorim.* **142** (2020), pp. 1145–1172.

[24] M. Enmark, M. Murugesan, H. Zhang, T. M. J. Nilsson, K. J. Kallio, A. Kamal and J. Liu, "Design and characterization of novel graphene-enhanced vapor chambers for lightweight and high-performance electronics cooling", *Nanotechnology* **36** (2025), article no. 105701.

[25] H. Singh, H. A. Budiarto, B. Singh, K. Kumar, R. Gupta, A. Bhowmik and A. J. Santhosh, "Graphene for next-generation technologies: Advances in properties, applica-

tions, and industrial integration", *Results Eng.* **27** (2025), article no. 106865.

[26] B. Du and Q. Jian, "Size controllable synthesis of graphene water nanofluid with enhanced stability", *Fuller. Nanotub. Carbon Nanostruct.* **27** (2018), pp. 87–96.

[27] P. Maheshwary, P. Belkhode, S. Shelare, D. P. Barai and B. A. Bhanvase, "Nanofluids for manufacturing", in *Towards Nanofluids for Large-Scale Industrial Applications*, Elsevier Science, 2024, pp. 249–265.

[28] I. Razzaq, W. Xinhua, G. Rasool, et al., "Nanofluids for advanced applications: A comprehensive review on preparation methods, properties, and environmental impact", *ACS Omega* **10** (2025), pp. 5251–5282.

[29] X. Wang, G. Wang and L. Zhang, "Green and simple production of graphite intercalation compound used sodium bicarbonate as intercalation agent", *BMC Chem.* **16** (2022), article no. 13.

[30] A. R. I. Ali and B. Salam, "A review on nanofluid: preparation, stability, thermophysical properties, heat transfer characteristics and application", *SN Appl. Sci.* **2** (2020), article no. 1636.

[31] M. Tawalbeh, I. Shomope and A. Al-Othman, "Comprehensive review on non-Newtonian nanofluids, preparation, characterization, and applications", *Int. J. Thermofluids* **22** (2024), article no. 100705.

[32] A. K. Patra, M. K. Nayak and A. Misra, "Viscosity of nanofluids—A review", *Int. J. Thermofluid Sci. Technol.* **7** (2020), no. 2, article no. 070202.

[33] J. P. Meyer, S. A. Adio, M. Sharifpur and P. N. Nwosu, "The viscosity of nanofluids: A review of the theoretical, empirical, and numerical models", *Heat Transfer Eng.* **37** (2015), pp. 387–421.

[34] P. C. Mishra, S. Mukherjee, S. K. Nayak and A. Panda, "A brief review on viscosity of nanofluids", *Int. Nano Lett.* **4** (2014), pp. 109–120.

[35] J. T. Awua, "Influence of volume concentration and temperature on viscosity and thermal conductivity of Terminalia Superba (Afara) tree bark nanofluid", *Int. J. Sci. Res. (IJSR)* **12** (2023), pp. 2593–2598.

[36] V. N. Deshmukh, S. Radhakrishnan and R. R. Kulkarni, "Investigations on thermal conductivity, heat transfer coefficient and viscosity of graphite nanoparticle dispersed nanofluid", *J. Nanofluids* **6** (2017), pp. 1008–1016.

[37] J. Pashikanti and D. R. Susmitha Priyadharshini, "Influence of variable viscosity on entropy generation analysis due to graphene oxide nanofluid flow", *J. Nanofluids* **12** (2023), pp. 1360–1373.

[38] B. Wright, D. Thomas, H. Hong and P. Smith, "Time dependent thermal conductivities of nanofluids containing carbon nanotubes and metal oxides", *J. Nanofluids* **2** (2013), pp. 45–49.

[39] N. Salemi, S. M. Abtahi, M. Rowshanzamir and S. M. Hejazi, "Surface tension and viscosity of nanofluids containing various nanoparticles", *Mater. Focus* **6** (2017), pp. 698–704.

[40] V. Kugarajah, A. K. Ojha, H. Hadem, N. Dasgupta, B. N. Mishra, S. Ranjan and S. Dharmalingam, "Nanoparticles and nanofluids: Characteristics and behavior aspects", in *Food, Medical, and Environmental Applications of Nanomaterials*, Elsevier, 2022, pp. 41–71.

[41] S. K. Rawat, M. Yaseen, A. Shafiq, M. Kumar and Q. M. Al-Mdallal, "Nanoparticle aggregation effect on nonlinear convective nanofluid flow over a stretched surface with linear and exponential heat source/sink", *Int. J. Thermofluids* **19** (2023), article no. 100355.

[42] G. Yalçın, S. Öztuna, A. S. Dalkılıç and S. Wongwises, "Effect of particle size on SiO_2 nanofluid viscosity determined by a two-step method", *J. Therm. Anal. Calorim.* **149** (2024), pp. 13681–13696.

[43] M. Klazly and G. Bognár, "A novel empirical equation for the effective viscosity of nanofluids based on theoretical and empirical results", *Int. Commun. Heat Mass Transfer* **135** (2022), article no. 106054.

[44] T. Gaudin and H. Ma, "The macroscopic viscosity approximation: A first-principle relationship between molecular diffusion and viscosity", *AIP Adv.* **10** (2020), article no. 035311.

[45] A. Ahmadi Nadooshan, H. Eshgarf and M. Afrand, "Evaluating the effects of different parameters on rheological behavior of nanofluids: A comprehensive review", *Powder Technol.* **338** (2018), pp. 342–353.

[46] J. Liao, S. Qing, X. Zhang, X. Huang and X. Wang, "Factors that influence the aggregation structure of nanoparticles in nanofluids: A molecular dynamics simulation", *J. Mol. Liq.* **368** (2022), article no. 120716.

[47] S. Kumar Rawat, M. Yaseen, U. Khan, et al., "Insight into the significance of nanoparticle aggregation and non-uniform heat source/sink on titania–ethylene glycol nanofluid flow over a wedge", *Arab. J. Chem.* **16** (2023), article no. 104809.

[48] I. Akande, T. Bridgwater, P. J. van Koningsbruggen and Q. Yuan, "Advances in the modelling of concentration-dependent relative viscosity data for nanofluids by introducing the Dispersion Factor", *J. Mol. Liq.* **380** (2023), article no. 121644.

[49] F. Duan, D. Kwek and A. Crivoi, "Viscosity affected by nanoparticle aggregation in Al_2O_3-water nanofluids", *Nanoscale Res. Lett.* **6** (2011), article no. 248.

[50] K. Ramachandran, K. Kadirgama, O. I. Awad, D. Ramasamy, M. Samykano and W. H. Azmi, "Comprehensive review of principle factors for thermal conductivity and dynamic viscosity enhancement in thermal transport applications: An analytical tool approach", *Int. Commun. Heat Mass Transfer* **98** (2018), pp. 13–21.

[51] H. A. Moghaddam, A. Ghafouri and R. Faridi Khouzestani, "Viscosity and thermal conductivity correlations for various nanofluids based on different temperature and nanoparticle diameter", *J. Braz. Soc. Mech. Sci. Eng.* **43** (2021), article no. 303.

[52] M. Baratpour, A. Karimipour, M. Afrand and S. Wongwises, "Effects of temperature and concentration on the viscosity of nanofluids made of single-wall carbon nanotubes in ethylene glycol", *Int. Commun. Heat Mass Transfer* **74** (2016), pp. 108–113.

[53] O. Vergote, I. Bellemans, A. Van den Bulck, M. Shevchenko, R. Starykh, E. Jak and K. Verbeken, "Viscosity experiments of slag-spinel suspensions: The effect of volume fraction, particle size, and shear rate", *J. Rheol.* **67** (2023), pp. 1159–1174.

[54] V. Y. Rudyak, "Viscosity of nanofluids. Why it is not described by the classical theories", *Adv. Nanoparticles* **2** (2013), pp. 266–279.

[55] Z. Wenhao, "Influence of temperature and concentration on viscosity of complex fluids", *J. Phys.: Conf. Ser.* **1965** (2021), article no. 012064.

[56] Y.-M. Chen and A. J. Pearlstein, "Onset of convection in variable viscosity fluids: Assessment of approximate viscosity–temperature relations", *Phys. Fluids* **31** (1988), pp. 1380–1385.

[57] P. K. Namburu, D. P. Kulkarni, D. Misra and D. K. Das, "Viscosity of copper oxide nanoparticles dispersed in ethylene glycol and water mixture", *Exp. Thermal Fluid Sci.* **32** (2007), pp. 397–402.

[58] H. Li, L. Wang, Y. He, Y. Hu, J. Zhu and B. Jiang, "Experimental investigation of thermal conductivity and viscosity of ethylene glycol based ZnO nanofluids", *Appl. Therm. Eng.* **88** (2015), pp. 363–368.

[59] X. Hu, D. Yin, X. Chen and G. Xiang, "Experimental investigation and mechanism analysis: Effect of nanoparticle size on viscosity of nanofluids", *J. Mol. Liq.* **314** (2020), article no. 113604.

[60] H. D. Koca, S. Doganay, A. Turgut, I. H. Tavman, R. Saidur and I. M. Mahbubul, "Effect of particle size on the viscosity of nanofluids: A review", *Renew. Sust. Energ. Rev.* **82** (2018), pp. 1664–1674.

[61] N. Ahammed, L. G. Asirvatham and S. Wongwises, "Effect of volume concentration and temperature on viscosity and surface tension of graphene–water nanofluid for heat transfer applications", *J. Therm. Anal. Calorim.* **123** (2015), pp. 1399–1409.

[62] D. Gaber, M. Abu Haija, A. Eskhan and F. Banat, "Graphene as an efficient and reusable adsorbent compared to activated carbons for the removal of phenol from aqueous solutions", *Water Air Soil Pollut.* **228** (2017), article no. 320.

[63] A. A. Alhwaige, S. M. Alhassan, M. S. Katsiotis, H. Ishida and S. Qutubuddin, "Interactions, morphology and thermal stability of graphene-oxide reinforced polymer aerogels derived from star-like telechelic aldehyde-terminal benzoxazine resin", *RSC Adv.* **5** (2015), pp. 92719–92731.

[64] Y.-R. Lee, J.-X. Huang, J.-C. Lin and J.-R. Lee, "Study of the substrate-induced strain of as-grown graphene on Cu(100) using temperature-dependent Raman spectroscopy: Estimating the mode Grüneisen parameter with temperature", *J. Phys. Chem. C* **121** (2017), pp. 27427–27436.

[65] D. Kostiuk, M. Bodik, P. Siffalovic, et al., "Reliable determination of the few-layer graphene oxide thickness using Raman spectroscopy", *J. Raman Spectrosc.* **47** (2015), pp. 391–394.

[66] L. Yu, L. Wang, W. Xu, L. Chen, M. Fu, J. Wu and D. Ye, "Corrigendum to 'Adsorption of VOCs on reduced graphene oxide' [J. Environ. Sci. 67 (2018) 171–178]", *J. Environ. Sci.* **90** (2020), p. 408.

[67] M. Makhlouf, S. Bouriche, Z. Benmaamar and D. Villemin, "Electromagnetic shielding properties of polymer blended with graphene sheets and iron oxide particles", *J. Renew. Energies* **28** (2025), pp. 135–150.

[68] F. Wang, L. Han, Z. Zhang, X. Fang, J. Shi and M. Ma, "Surfactant-free ionic liquid-based nanofluids with remarkable thermal conductivity enhancement at very low loading of graphene", *Nanoscale Res. Lett.* **7** (2012), article no. 314.

[69] Y. Wang, H. A. I. Al-Saaidi, M. Kong and J. L. Alvarado, "Thermophysical performance of graphene based aqueous nanofluids", *Int. J. Heat Mass Transfer* **119** (2018), pp. 408–417.

[70] E. Sadeghinezhad, M. Mehrali, M. A. Rosen, A. R. Akhiani, S. T. Latibari, M. Mehrali and H. S. C. Metselaar, "Experimental investigation of the effect of graphene nanofluids on heat pipe thermal performance", *Appl. Therm. Eng.* **100** (2016), pp. 775–787.

[71] M. Mehrali, E. Sadeghinezhad, S. T. Latibari, S. N. Kazi, M. Mehrali, M. N. B. M. Zubir and H. S. C. Metselaar, "Investigation of thermal conductivity and rheological properties of nanofluids containing graphene nanoplatelets", *Nanoscale Res. Lett.* **9** (2014), article no. 15.

[72] S. Iranmanesh, M. Mehrali, E. Sadeghinezhad, B. C. Ang, H. C. Ong and A. Esmaeilzadeh, "Evaluation of viscosity and thermal conductivity of graphene nanoplatelets nanofluids through a combined experimental–statistical approach using respond surface methodology method", *Int. Commun. Heat Mass Transfer* **79** (2016), pp. 74–80.